Proceedings of The Fifteenth (2005) International Offshore and Polar Engineering Conference
Seoul, Korea, June 19–24, 2005

ISBN 1-880653-64-8 (Set); ISSN 1098-6189 (Set)

Interaction of Forces on Caissons in Undrained Soils

H. A. Taiebat
Faculty of Engineering, University of Technology, Sydney, Australia
J. P. Carter
Department of Civil Engineering, The University of Sydney, Australia

ABSTRACT

In this paper the results of a numerical study on the behaviour of caisson foundations subjected to various combinations of loading are presented. A typical caisson has been used in this study with a length-to-diameter ratio of 2. The caisson is assumed to be embedded in a homogeneous soil deforming under undrained conditions. The performance of the caisson under separate axial, lateral and torsional forces was investigated first, followed by the interaction of these forces with each other. The ultimate capacity of the caisson under combined loading is presented in the form of failure envelope in the axial-torsional loading plane and axial-lateral, and lateral-torsional loading surfaces along the skirt of the foundation. It is shown that, although lateral capacity of the caisson is dependent on the location of the padeye, a unique normalised failure surface can be used to represent the capacity of the caisson under all combinations of axial, lateral and torsional loads regardless of the location of the padeye.

KEY WORDS: Caisson foundations; undrained soils; failure envelope, finite element analysis.

.NTRODUCTION

Both the exploration and exploitation of hydrocarbons are heading into deeper waters. Tension leg, taut and semi-taut leg and semi-submersible platforms are among the options that are used increasingly in deep waters. With the greater water depths there are greater needs for more robust anchoring systems to transfer predominantly tensile and lateral forces to the ocean floor. Tension leg platforms are floating structures anchored by pretensioned tendons which exert considerable vertical forces, ranging up to 27 MN, on the foundation. Laterally moored systems, such as Spars, have the dominant load in the horizontal direction, in the order of 9 MN (Sukumaran et al., 1999). The foundation systems suitable for platforms in deep and ultra deep waters include traditional driven piles, drag anchors and suction caissons.

Caisson foundations have been increasingly used over the last two decades in marine environments for temporary or permanent mooring of floating offshore facilities, tension leg platforms as well as gravity based structures. Recently, their use has also been proposed for foundations of offshore wind turbines (Houlsby & Byrne, 2000, Byrne et al., 2002). They are considered as particularly reliable and cost-effective alternatives to more conventional mooring systems, such as pile foundations, in deep and ultra deep waters.

Caissons or bucket foundations are hollow cylindrical structures with a top cap and a relatively thin skirt usually made of steel or concrete. Caisson foundations have typically a large diameter and a wide range of length-to-diameter ratio, so they provide relatively large lateral and axial capacities. Their large load capacity and the efficiency of their installation are the main advantages of caissons over other conventional offshore anchoring systems. A caisson can partially penetrate into the seabed under its own weight. Further penetration is usually facilitated by pumping water out of the caisson chamber, thus applying suction inside the caisson. The difference between the external and internal fluid pressures acts as an external surcharge, pushing the caisson into the soil. This simple installation procedure is probably the greatest advantage of caisson foundations over pile foundations. A suction caisson can be withdrawn later by applying a positive pressure inside the chamber to assist in pulling it out of the soil.

In the marine environment caisson foundations are subjected to all combinations of axial, lateral and torsional loading. As part of a mooring system, a caisson foundation is predominantly subjected to axial uplift and lateral loading, transferred from a mooring line to a padeye attached to the caisson wall. Any misalignment of the padeye or change in the direction of the mooring line also applies torsional loads to the caisson. Significant rotational loading is also expected when caissons are used to support tall structures subjected to large eccentrically applied horizontal forces, such as modern wind turbines.

The response of caisson foundations to axial and lateral loads has been studied extensively in the past. The focus of some earlier works (e.g., Bransby & Randolph, 1997, 1998, Bransby & Martin, 1999) has been on the capacity mobilized at the tip of caissons, ignoring the resistance of its skirt. In other studies (e.g., Sukumaran et al., 1999, Zdravkovic et al., 2001, Deng & Carter, 1999, 2002, Deng et al., 2001) resistances of both the tip and the skirt of caissons have been considered. Randolph et al. (1998) presented an upper bound model for calculation of the

uplift capacity of suction caissons, adding new features to the upper bound solution introduced by Murff and Hamilton (1993) for the undrained capacity of laterally loaded piles. Aubeny et al. (2003) also presented upper bound solutions for caisson foundations subjected to inclined loadings. The effects of torsional loads on the axial and lateral capacities of caissons have been investigated by Taiebat & Carter (2004), where it was shown that, in general, torsional loads reduce the axial capacity and lateral resistance of cylindrical caissons. In addition to the above numerical and theoretical studies, experimental studies of suction caissons subjected to inclined loading have also been reported, in both small scale models and prototype caissons, by various researchers, including Anderson et al. (1993), Keaveny et al. (1994), Randolph et al. (1998), Watson et al. (2000), and Clukey et al. (2003).

In this paper the performance of a typical caisson foundation under the effects of combinations of axial, lateral and torsional forces is studied, and the interaction of these forces is presented in the form of failure envelopes. As the main aim of this study is to investigate the overall interaction of these forces, the problem was solved for only one typical caisson with a length-to-diameter (aspect) ratio of 2. This is within the range typically found in practice.

FINITE ELEMENT MODEL

The typical caisson foundation considered here has a diameter D and a length L = 2D, and is embedded in a homogeneous elastoplastic soil that deforms under undrained conditions. It was assumed that the soil obeys the Tresca failure criterion and has a uniform undrained shear strength s_u and an undrained Young's modulus $E_u = 300\,s_u$. A Poisson's ratio $\nu \approx 0.5$ (= 0.49) was assumed to approximate the constant volume response of the soil under undrained conditions. The rigidity index G/s_u is therefore equal to 100, where G is the elastic shear modulus of the soil. The caisson material has a Young's modulus of $E_c = 1000\,E_u$.

The geometry of the problem under investigation is axi-symmetric, but generally the loading is of course non-symmetric. The axi-symmetric nature of the geometry was exploited to achieve economies in obtaining the finite element solutions. The finite element mesh used in the analyses has 12 wedges of elements in the circumferential direction. Each wedge of the typical caisson consists of 304 isoparametric (20 node) brick elements. A thin layer of elements has been used around and under the caisson in order to capture the effects of shearing close to the foundation. A schematic representation of six of the wedges, i.e., half of the three-dimensional finite element mesh used in the analyses of the typical caisson, is shown in Fig. 1, which also defines the overall geometry of the finite element model. Of course, a finer mesh may be used to obtain a more accurate finite element solution to the problem in hand. However, as the main aim of this study was to find the overall interaction of the forces at foundation failure, this finite element mesh was considered satisfactory.

The small strain formulation used for these analyses is based on the "semi-analytical" approach in finite element modelling described by Zienkiewicz & Taylor (1989), which is an efficient tool for three-dimensional problems. A semi-analytical finite element method, based on representation of nodal variables in terms of discrete Fourier series, has been integrated into the finite element code AFENA (Carter and Balaam, 1995). Application of this method in the analyses of three-dimensional problems has shown a considerable reduction in computational time, compared with a straightforward 3-D analysis. Details of the semi-analytical method used in this study may be found in Taiebat and Carter (2001).

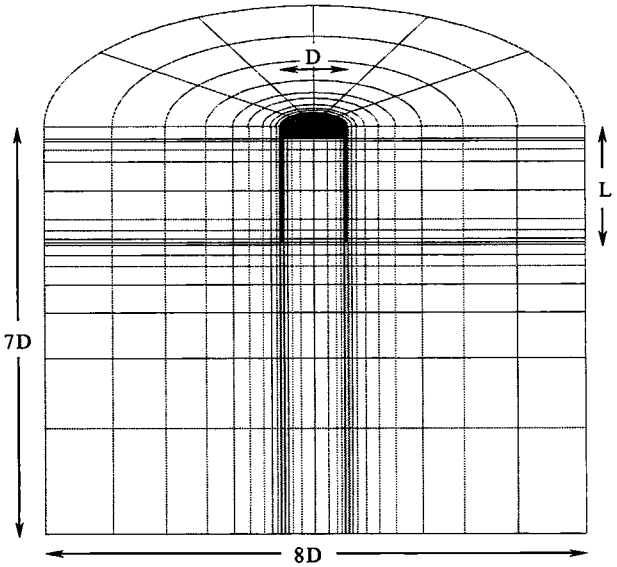

Fig. 1: Finite element mesh and geometry of the problem.

All analyses were performed under "displacement-defined" conditions, where a vertical or torsional displacement was applied to the foundation at the ground level, or a lateral displacement was applied at various locations along the skirt of the foundation below the ground level. A combination of two or three components of displacement was also applied to the foundation to investigate its behaviour under combined loading. It is assumed that the loads are applied at a rate sufficiently rapid so that the surrounding soil deforms under undrained conditions. No provision has been made to model any separation or de-bonding that may occur between the soil and the foundation.

The resistance of the caisson foundation under each individual component of loading, i.e., axial, lateral or torsional loading, is presented in the next section. The failure loads for the foundation under different combinations of loading have also been obtained and used to form failure envelopes in two-dimensional loading planes and three-dimensional loading space, which will be presented in subsequent sections.

RESISTANCE UNDER AXIAL LOADING

The axial capacity of a caisson foundation in undrained soil, V_u, can be approximated using the conventional method of bearing capacity calculation, e.g., from the equation suggested by Vesic (1975), as:

$$V_u = \zeta_s \,.\, \zeta_d \,.\, N_c \,.\, A \,.\, s_u \qquad (1)$$

where A is the plan area of the caisson, N_c is the bearing capacity factor for a strip footing corresponding to the undrained shear strength of the soil, ζ_s and ζ_d are factors that include the effects of the shape of the footing and the effects of embedment of the foundation. The bearing capacity factor for undrained soil is $N_c = (2+\pi)$. The shape factor for a circular footing is usually suggested as $\zeta_s = 1.2$. The embedment factor for a circular footing has been suggested as $\zeta_d = 1 + 0.4\tan^{-1}(L/D)$ (Vesic, 1975); for L/D = 2 the embedment factor is $\zeta_s = 1.443$. Therefore, for the special cases considered here the axial load capacity of a buried circular footing is given by the conventional method (Eq. 1) as $V_u = 8.9\,A\,s_u$. The effects of the adhesion developed on the caisson skirt are not included in this method.

Deng and Carter (1999) recognised the effect of adhesion developed on the skirt of the foundation and suggested an equation for the uplift capacity of caisson foundations in an undrained homogeneous soil as:

$$V_u = N_p \cdot \zeta_s \cdot \zeta_{ce} \cdot A \cdot s_u \quad (2)$$

Based on the results of a series of finite element analyses, Deng and Carter (1999) recommended a value for the uplift capacity factor as $N_p \approx 9.0$ and an embedment factor $\zeta_{ce} = 1 + 0.4\,(L/D)$. Eq. 2 results in an uplift capacity of $19.44\,A\,s_u$ for caissons with L/D = 2.

It should be noted that the problem of uplift capacity of a caisson in soil deforming under undrained conditions is essentially a reverse bearing capacity problem and can be treated similarly (e.g., Anderson *et al*, 1993). Therefore, Eq. 2 may equally be used to calculate the uplift capacity and the compressive bearing capacity of caisson foundations. The results of the finite element analysis do not indicate any significant change in the axial capacity when the direction of loading is reversed.

The result of the finite element analysis of the typical caisson under axial load is presented in Fig. 2. The response is approximately linear at the beginning of loading where about 65% of the ultimate axial resistance is mobilized. After a rapid bend in the load-deflection curve, the rate of increase in the resistance reduces significantly. At a relatively large displacement the increase in the resistance becomes insignificant and the ultimate load is approached. The ultimate axial resistance of the caisson predicted by the finite element analysis, at a vertical displacement of about 50% of the caisson diameter, is $V_u = 18.4\,A\,s_u$. This value is slightly smaller than that predicted by Eq. 2, but very close to the upper bound solution presented by Aubeny et al. (2003), i.e., approximately $18.3\,A\,s_u$. If the skirt adhesion, $\pi D L s_u$, is added to the capacity predicted by the conventional method, Eq. 1, the result will be $16.9\,A\,s_u$, which is closer to the value predicted by the finite element analysis.

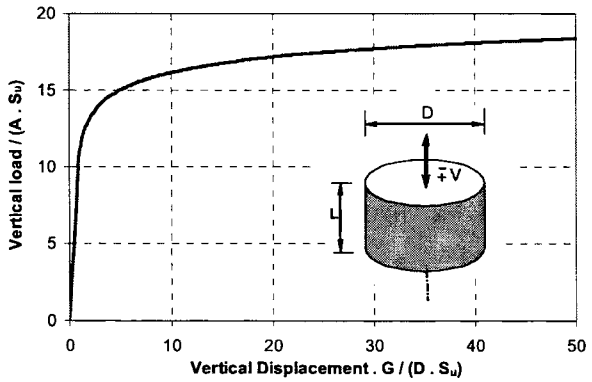

Fig. 2: Caisson response under axial loading.

RESISTANCE UNDER TORSIONAL LOADING

Assuming the full value of the undrained shear strength of the soil is mobilized as a shear stress at the caisson-soil interface, the theoretical value for the ultimate torsional capacity of a caisson foundation, T_u, can be calculated as the sum of the base resistance and the shaft resistance, i.e.,

$$T_u = s_u \pi D^2 \left(\frac{L}{2} + \frac{D}{12} \right) \quad (3)$$

Eq. 3 gives the ultimate torsional capacity of $3.402\,D^3\,s_u$ for the typical caisson considered here with L/D = 2.

The load deflection curve predicted by the finite element analysis of the caisson under torsional loading is presented in Fig. 3. The response is virtually elastic-perfectly-plastic. The torsional resistance increases linearly to its ultimate value at a rotation of about 0.006 radians, after which the resistance remains constant. The ultimate torsional resistance predicted by the finite element analysis is $T_u = 3.40\,D^3\,s_u$, in excellent agreement with the theoretical value obtained using Eq. 3.

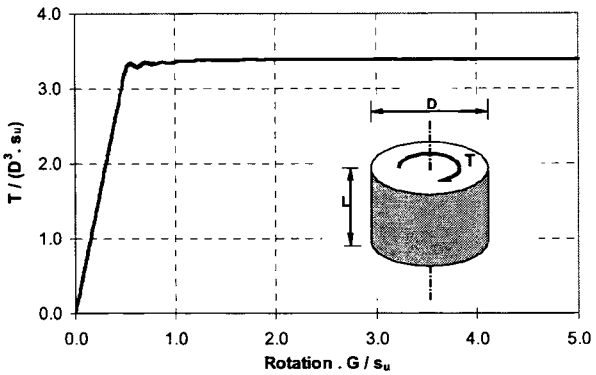

Fig. 3: Caisson response under torsional loading.

RESISTANCE UNDER LATERAL LOADING

The lateral resistance of a caisson foundation in an undrained homogeneous soil can be given as:

$$H_u = N_h \cdot L \cdot D \cdot s_u \quad (4)$$

where H_u is the ultimate lateral capacity of the caisson and N_h is defined as the lateral capacity factor. Deng and Carter (1999) suggested an expression for the lateral capacity factor that is a function of the point where the load is applied. It was noted that the aspect ratio of the caisson, L/D, has no significant effect on the lateral capacity factor N_h. The expression for the lateral capacity factor was derived using a curve fitting method applied to the results of a comprehensive series of finite element analyses of caissons with different aspect ratios and padeye locations. For lateral load applied at ground level, at a depth of 0.6L, and at the tip of the caisson, the lateral capacity factors suggested by Deng and Carter (1999) are $N_h = 4.8$, 11.66 and 7.0, respectively. The lateral capacity factors obtained by the upper bound solution of Aubeny et al. (2003) are approximately 4.5, 11.1 and 5.5 for lateral loads applied at the ground level, at 0.5L, and at the tip of the caisson skirt, respectively.

The results of the finite element analysis of the caisson subjected to lateral loading applied at the ground level are presented in Fig. 4. A lateral capacity factor of $N_h = 4.0$ is obtained for this case. For lateral loads applied at 0.6L below the ground and at the tip of the caisson skirt, lateral capacity factors of 10.7 and 5.3 are predicted by the finite element analyses. These values are smaller than those suggested by Deng and Carter (1999) and by Aubeny et al. (2003).

The lateral resistance of a caisson depends on the location of the padeye, as any eccentricity of the lateral load applies an overturning moment on the caisson. The variation of the lateral resistance of the caisson with the point of load application is presented in Fig. 5. In this figure "d" represents the depth of the padeye. The response of the

caisson considered here is very similar to those reported by Deng and Carter (1999) and Aubeny et al. (2003). The maximum lateral resistance occurs when the lateral load is applied at about 0.6L below the ground level. The lateral capacity factor is also a function of the aspect ratio of the caisson, L/D. As the aspect ratio increases the lateral capacity factor increases slightly as shown by Aubeny el al. (2003).

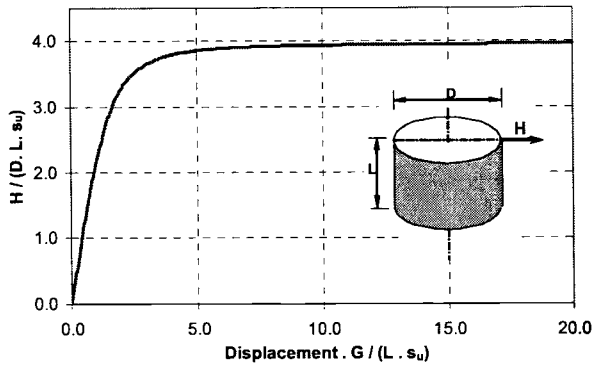

Fig. 4: Caisson response under lateral loading.

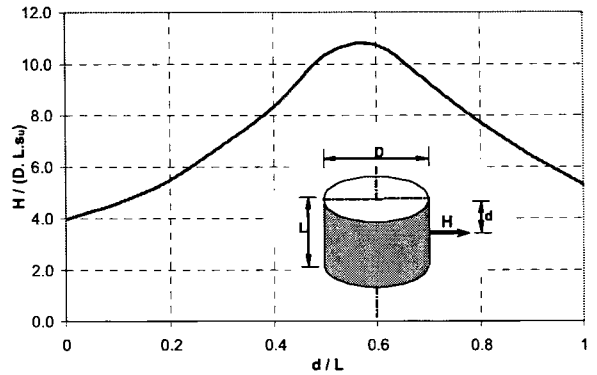

Fig. 5: Lateral resistance versus the load application point.

FAILURE ENVELOPES

In order to evaluate the interaction between different components of oading, a series of finite element analyses was performed using different ratios of the vertical and lateral displacements and rotation of the caisson. For each loading case "failure" was assumed if any of the following deformations occurred; a vertical displacement equal to about 50% of the diameter of the caisson, a lateral displacement equal to approximately 20% of the diameter, and a twisting rotation of 0.4 radians. As an example the predicted response of the caisson under a combination of axial and torsional deformations is presented in Fig. 6. For this case a fixed ratio of a twisting rotation and an axial displacement was applied to the foundation incrementally. Generally there is a sharp increase in the torsional resistance at the beginning of the loading. The torsional resistance decreases and then remains constant at later stages of the loading. The axial load-displacement curve is approximately linear at the beginning of loading where about 2/3 of the axial resistance is mobilized. After that the rate of increase in the axial resistance reduces and eventually becomes insignificant at the point where failure is assumed to occur.

The results of the finite element analyses will be presented in the following sections in the form of failure loci in axial-lateral, axial-torsional, lateral-torsional loading planes, followed by a generalized non-dimensional 3-D failure surface.

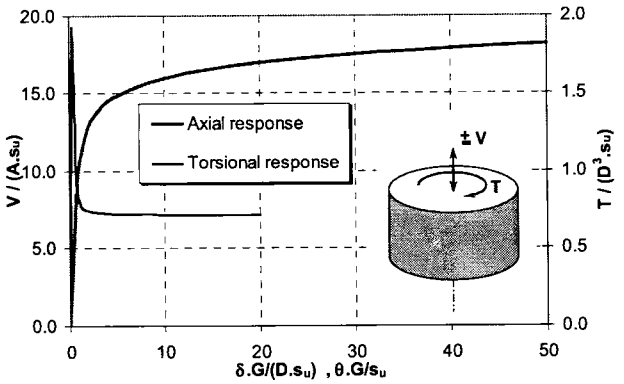

Fig. 6: Caisson response under a combination of axial and torsional deformations.

AXIAL-LATERAL FAILURE ENVELOPES

The results of a series of finite element analyses of the caisson subjected to different combinations of axial and lateral loads applied at three locations along the caisson skirt are presented in Fig. 7. Each curve shows the locus of the failure points for the caisson obtained at a specific padeye depth. In this figure "α" represents the inclination angle of the resultant load applied at the centre line of the caisson at failure. The inclination angle is measured with the horizontal. It may be seen that the inclination of the load has a greater effect in reducing the axial capacity if the load is applied at the ground level or at the tip of the caisson skirt. An inclination of 45° for a load applied at ground level reduces the axial capacity of the caisson to half of its value under pure axial loading, while the same inclination reduces the axial capacity of the caisson by only 5% if the load is applied at d/L = 0.6. The failure envelopes obtained by the numerical analysis and presented in Fig. 7 are all lie inside the failure envelopes predicted by the upper bound solutions of Aubeny et al. (2003).

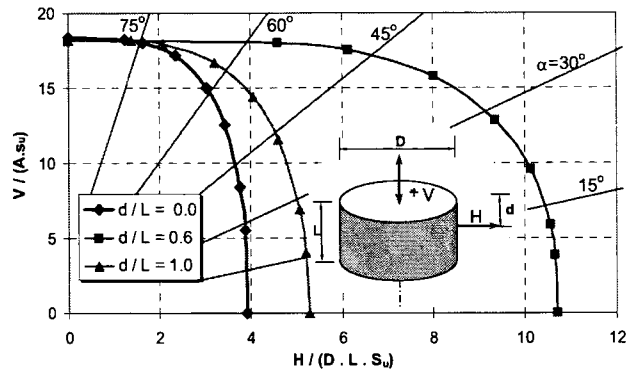

Fig. 7: Failure loci in axial-lateral loading plane.

As explained previously, the lateral capacity of the caisson depends on the point of application of the load. A schematic representation of the shape of the axial-lateral failure surface along the skirt of the caisson is shown in Fig. 8. The failure surface bulges in the vicinity of d/L = 0.6, where the maximum lateral capacity is mobilized.

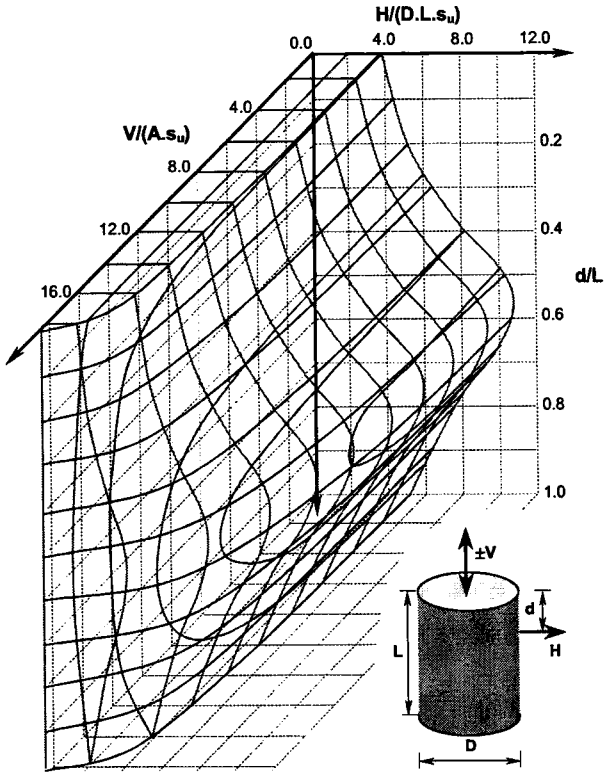

Fig. 8: Schematic representation of the failure surface along the caisson skirt in axial-lateral loading planes.

Non-dimensional forms of the failure loci in the axial-lateral loading plane can be obtained using the maximum axial capacity, V_{max}, and the maximum lateral capacity at any padeye location, H_{max}, as the normalisation factors. These non-dimensional failure loci are presented in Fig. 9. It can be seen that all the failure loci are very close to each other and the discrepancies between different failure loci are virtually insignificant. Therefore it may be concluded that, for most practical purposes and for any caisson, a unique normalised failure locus in the axial-lateral loading plane can be found which is representative of all failure loci for the caisson with various padeye locations. Furthermore, this failure locus may also be applicable to caissons with other aspect ratios, although this point warrants further investigation.

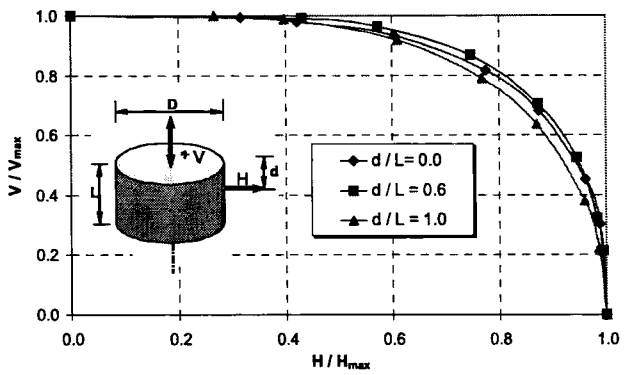

Fig. 9: Non-dimensional failure loci in axial-lateral loading plane.

AXIAL-TORSIONAL FAILURE PLANE

A failure locus for the caisson subjected to combinations of axial and torsional forces is presented in Fig. 10, which shows that torsional forces have significant effects on the axial capacity of the caisson. When much of the shearing strength around and under the caisson is mobilized by torsion, the axial capacity of the foundation reduces significantly. Torsional displacements govern the failure mechanism of the foundation for axial loads lower than about $0.6\,V_{max}$.

The effects of torsion can best be viewed in Fig. 11, where the ultimate axial capacity of the caisson is shown in terms of the inclination angle, β, of a pair of loads applied at the outer boundary of the caisson. The inclination of a pair of loads to the vertical induces rotation of the caisson while the net lateral force is zero. The inclination angle can be calculated as: $\beta = \tan^{-1}(2.T/D.V)$. Inclination angles less than 10° do not have a significant effect on the axial resistance of the foundation. However, at larger inclination angles the effects become very significant. An inclination angle of $\beta = 45°$ reduces the axial capacity of the caisson to half of its maximum value under pure vertical loading.

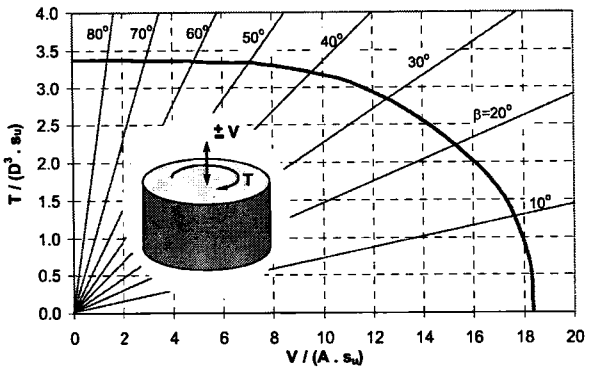

Fig. 10: Failure locus in axial-torsional loading plane.

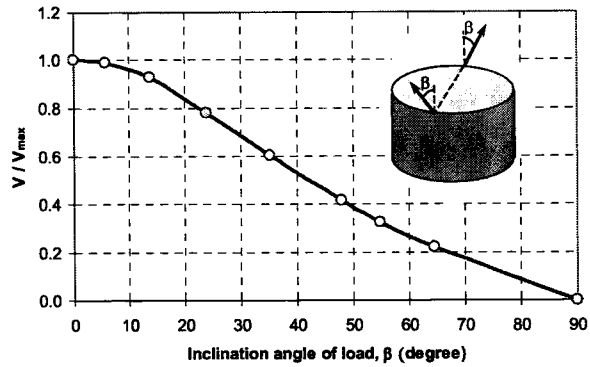

Fig. 11: Effects of load inclination on the ultimate axial capacity.

A normalised form of the failure locus in the axial-torsional loading plane is also presented in Fig. 12. In this figure, the axial and torsional forces are normalised by their maximum values, V_{max} and T_{max}, obtained under either pure axial or pure torsional loading. It is noted that these are small strain results and in reality the ultimate axial capacity may increase slightly at larger vertical displacements.

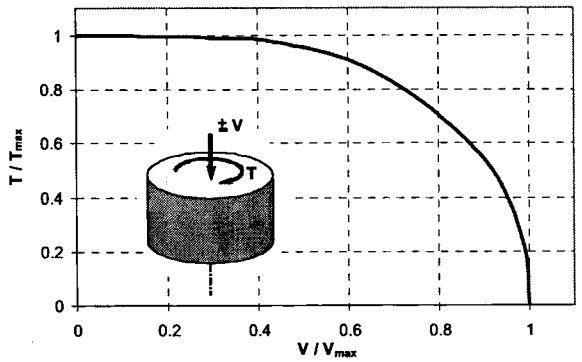

Figure 12: Non-dimensional failure locus in the axial-torsional loading plane.

LATERAL-TORSIONAL FAILURE PLANE

The responses of the caisson foundation to different combinations of lateral and torsional deformations are presented in Fig. 13 as failure loci for three different padeye locations along the caisson skirt. As mentioned before, any misalignment of the padeye induces torsional loads on the caisson. The angle of the misalignment, γ, is superimposed on the failure loci in Fig. 13. Misalignment in this case is due to the line of action of the applied lateral force not passing through the vertical axis of the cylindrical caisson. The effects of the misalignment of the padeye, γ, on the ultimate lateral capacity of the caisson can be best viewed in Fig. 14, which shows that the maximum reduction in the ultimate lateral capacity occurs when the padeye is located at about 0.6L below the ground line. At this point the lateral capacity of the caisson reduces to about 32% of its capacity under pure lateral load under a padeye misalignment of $\gamma = 90°$. When the padeye is located at the top of the caisson, the maximum reduction in the ultimate lateral capacity is about 23%. For a practical range of padeye misalignment, which is normally below 25°, the reductions in the lateral capacity are about 3%, 30% and 5% for padeye located at the top, at d/L = 0.6 and at the tip of the skirt, respectively. It may be noticed that the reduction in the ultimate lateral capacity of the caisson is dependent on both the angle of misalignment and the location of the padeye.

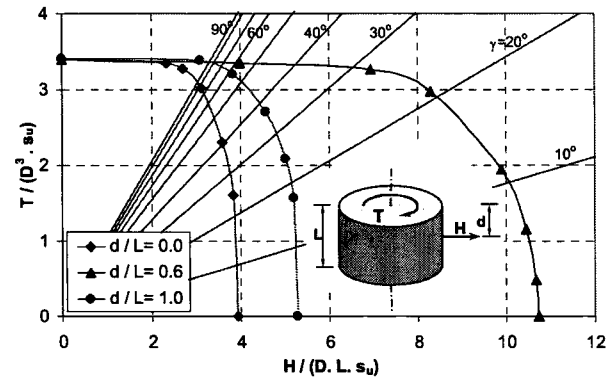

Figure 13: Failure locus in the lateral-torsional loading plane.

A schematic representation of the failure surface along the skirt of the caisson is shown in Fig. 15. The failure surface bulges up in the direction of the lateral load axis in the vicinity of d/L = 0.6, where the maximum lateral capacity is mobilized.

Normalised forms of the failure envelopes in the lateral-torsional loading plane are shown in Fig. 16, where the ultimate torsional and lateral forces are normalised with their maximum values, T_{max} and H_{max}, obtained under pure torsional and pure lateral loading at the different padeye locations. Fig. 16 shows that as the torsional force increases to its maximum value, the lateral resistance of the foundation decreases to about 60% of its maximum value. For the lateral loads lower than about 0.6 H_{max}, torsional displacements govern the failure mechanism of the caisson foundation.

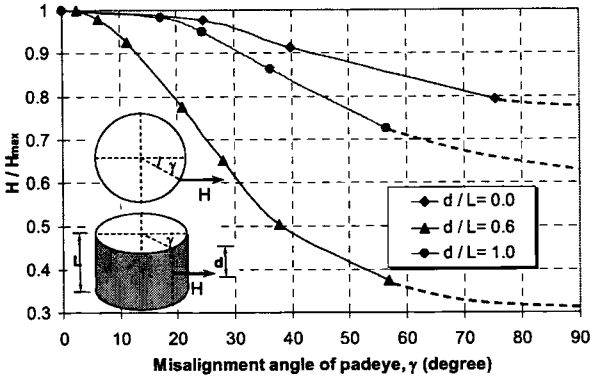

Fig. 14: Effects of padeye misalignment on the ultimate lateral capacity.

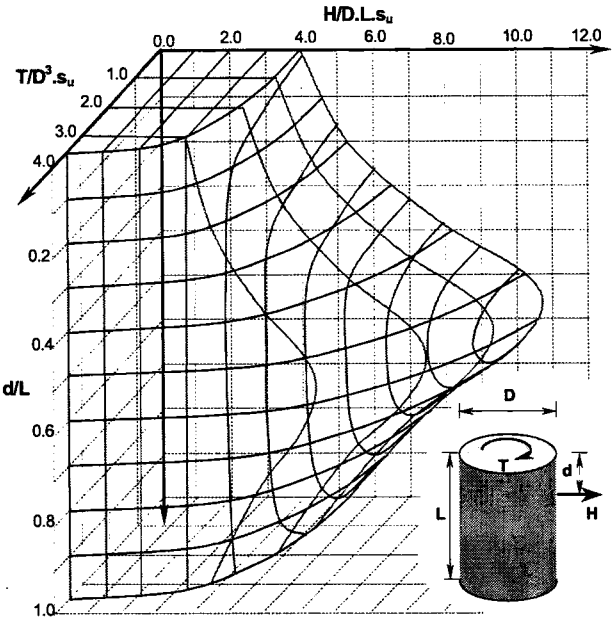

Fig. 15: Schematic representation of the failure surface along the caisson skirt in the lateral-torsional loading planes.

AXIAL-LATERAL-TORSIONAL FAILURE SURFACE

A series of finite element analyses was performed of the typical caisson in order to obtain a general failure surface for the foundation. Various combinations of axial, lateral and torsional displacements were applied to the foundation. In all analyses horizontal loads were applied at the ground level, i.e., at d/L = 0.

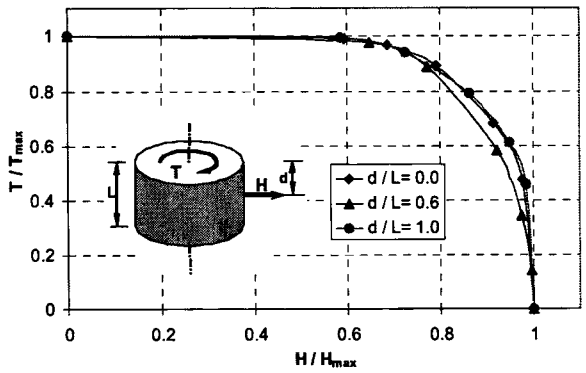

Figure 16: Non-dimensional failure loci in the lateral-torsional loading plane.

Representation of the failure loci in the axial-lateral-torsional loading space is shown in Fig. 17, where contours of equal torsional load are presented. Only 1/8 of the failure envelope is shown in Fig. 17, as it is symmetric with respect to all the three loading axes. In this figures all loads are normalised by their maximum values, V_{max}, H_{max} and T_{max}, obtained under pure axial, lateral and torsional loading, respectively. The failure loci presented in Fig. 17 were constructed based on a triangulation scheme of linear interpolation between computed failure points. The failure points are marked with small circles in Fig. 17.

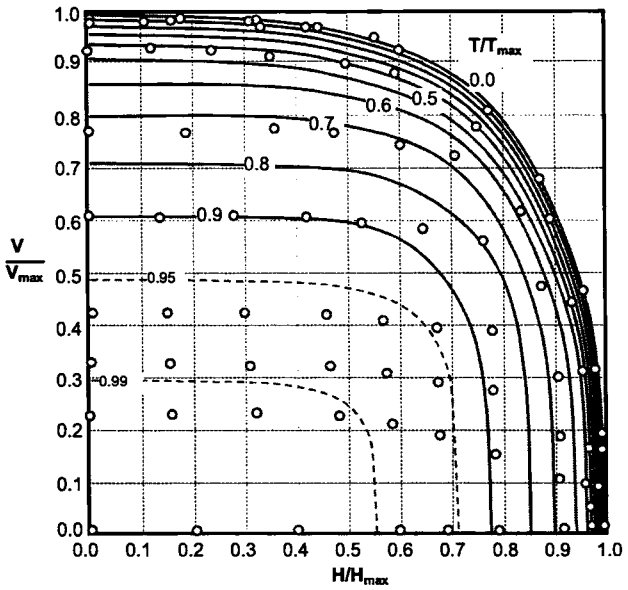

Figure 17: Failure loci in the non-dimensional VHT space.

A three-dimensional image of the failure envelope for the caisson in the axial-lateral-torsional loading space is presented in Fig. 18. Only half of the failure envelope is shown, as the uplift capacity problem of a caisson in clay soil deforming under undrained conditions is merely a reverse bearing capacity problem.

As shown in the previous sections, a single non-dimensional failure envelope in the axial-lateral or lateral-torsional loading planes can be obtained for the foundation regardless of the point of application of the lateral load. Therefore, the failure surface obtained for d/L = 0, and shown in Figs. 17 and 18, can be used for other values of d/L. Furthermore, the shapes of the failure surfaces for foundations with various aspect ratios are probably very similar to the non-dimensional three-dimensional failure surface shown in Figs. 17 and 18.

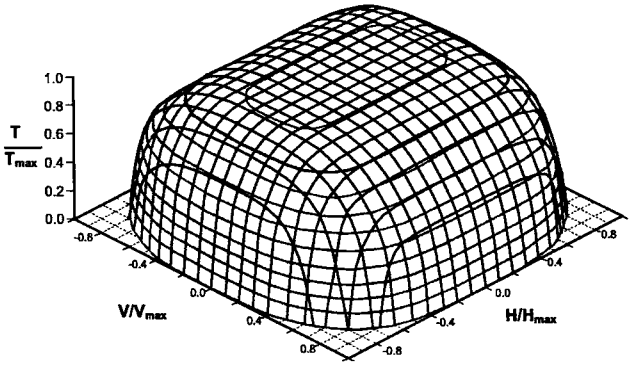

Figure 18: Three-dimensional failure envelope in non-dimensional load space.

CONCLUSIONS

This paper has presented the results of a numerical study of the capacity of a typical caisson foundation under various combinations of axial, lateral and torsional loads. The caisson was assumed to be embedded in a homogeneous soil which deforms under undrained conditions. The responses of the caisson under individual components of the loads were presented followed by its behaviour under combinations of these loads. It was shown that generally the torsional strength mobilizes at a faster rate compared with the lateral or axial strength of the caisson. Interactions of the loads on the foundation were presented in the form of failure envelopes in axial-lateral, axial-torsional and lateral-torsional loading planes.

It was shown that the inclination of an axial load has a greater effect in reducing the axial capacity if the load is applied at the ground level or at the tip of the caisson skirt. An inclination of 45° for a load applied at the ground level reduces the axial capacity to half of its value under pure axial loading, while the same inclination reduces the axial capacity of the caisson by only 5% if the load is applied at d/L = 0.6.

It was also shown that torsional forces have significant effects on the axial capacity of the caisson. For axial loads lower than about 0.6 V_{max}, torsional displacements govern the failure mechanism of the caisson foundation. An inclination angle of 45° for a pair of axial loads applied at the outer boundary of the caisson reduces the axial capacity to about half of its maximum value. This has a significant practical implication for installation or withdrawal of caisson foundations. Application of a torsional load can be used to reduce the risk of instability of the caisson that may occur under the large suctions normally required during the installation stage. Torsional loads can also facilitate the withdrawal of caisson foundations as they should reduce the active pressure required inside the caisson chamber.

Interactions of torsional-lateral forces show that the maximum reduction in the ultimate lateral capacity occurs when the padeye is located at 0.6L below the ground line. It was also noticed that the reduction in the ultimate lateral capacity of the caisson is a function of both the angle of load misalignment and the location of the padeye.

Failure envelopes were presented in non-dimensional forms and it has been shown that a single non-dimensional failure envelope can be obtained for the foundation in any of the different loading planes. This is a useful outcome of this study as it has significant practical implications. A normalised failure surface constructed for an arbitrary padeye location can be used to represent a generalized failure surface for the foundation and can be used for any other padeye location. Knowing the maximum resistance of a caisson foundation under purely axial, purely lateral and purely torsional loading applied at a particular padeye location, the resistance of the foundation against any combination of the axial, lateral and torsional loading can be obtained using the generalized failure surface. An example of a generalized failure surface for the caisson with L/D = 2 has been presented here. It is likely that this failure surface can also be used for caissons with other aspect ratios, however this point requires further investigation.

ACKNOWLEDGEMENT

The authors would like to acknowledge the support of the Centre for Built Infrastructure Research at the University of Technology Sydney, the Centre for Geotechnical Research at the University of Sydney, and the Australian Research Council's Special Research Centre for Offshore Foundation Systems.

REFERENCES

Anderson, K. H., Dyvik, R., Schoder, K., Hansteen, O. E., & Bysveen, S. 1993. Field test of anchors in clay, II: Prediction and interpretation. *Journal of Geotechnical Engineering, ASCE.* 119, 532-1549.

Aubeny, C. P., Han, S. W. & Murff, J. D. 2003. Inclined load capacity of suction caissons. *Int. J. for Numerical & Analytical Methods in Geomechanics.* 27, 1235-1254.

Bransby, M. F. & Randolph, M. F. 1997. Finite element modelling of skirted strip footings subjected to combined loadings. *Proc. 7th Int. Offshore and Polar Engineering Conference.* Honolulu, 791-796.

Bransby, M. F. & Randolph, M. F. 1998. Combined loading of skirted foundations. *Géotechnique.* **48**, 5, 637-655.

Bransby, M. F. & Martin, C. M. 1999. Elasto-plastic modelling of bucket foundations. *Proc. NUMOG VII.* Graz, 425-430.

Byrne, B., Houlsby, G., Martin, C. & Fish, P. 2002. Suction caisson foundations for offshore wind turbines. *Wind Engineering.* **26**, 3, 145-155.

Byrne, B., Houlsby, G. 2004. Experimental investigations of the response of suction caissons to transient combined loading.. *J. Geotch. & Geoen. Eng., ASCE.* 240-253.

Carter J. P. & Balaam N. P. 1995. *AFENA user's manual.* Version 5, Centre for Geotechnical Research, The University of Sydney, Australia.

Clukey, E.C., Aubeny, C.P. & Murff, J.D. 2003. Comparison of analytical and centrifuge model tests for suction caissons subjected to combined loads. *22nd International Conference on Offshore and Arctic Engineering,* Mexico, OMAE2003-37503.

Deng, W. & Carter, J., P. 1999. *Analysis of suction caissons in uniform soils subjected to inclined uplift loading.* Report No. R798, Department of Civil Engineering, The University of Sydney, Australia.

Deng, W., Carter, J. P. & Taiebat, H. A. 2001. Prediction of the Lateral Capacity of Suction Caissons, Keynote Lecture, *Proc.10th Int. Conference on Computer Methods and Advances in Geomechanics*, 1, 33-38.

Deng, W. & Carter, J. P. 2002. A theoretical study of the vertical uplift capacity of suction caissons. *Int. J. of Offshore and Polar Engineering.* 12, 2, 89-97.

Houlsby, G. & Byrne, B., 2000. Suction caisson foundations for offshore wind turbines and anemometer masts. *Wind Engineering.* **24**, 4, 249-255.

Keaveny, J., Hansen, S. B., Madshus, C. & Dyvik, R. 1994. Horizontal capacity of large-scale model anchors. *Proc. 13th Int. Conference on Soil Mechanics and Foundation Engineering.* New Delhi, 2, 977-680.

Murff, J. D. & Hamilton, J. M. 1993. P-ultimate for undrained analysis of laterally loaded piles. *Journal of Geotechnical Engineering, ASCE.* 119, 91-107

Randolph, M. F., O'Neill, M. P. & Erbrich, C. 1998. Performance of suction anchors in fine-grained calcareous soils. *Proc. Offshore Technology Conference, OTC 8831*, Houston, 521-529

Sukumaran, B., McCarron, W. O., Jeanjean, P. & Abouseeda, H. 1999. Efficient finite element techniques for limit analysis of suction caissons under lateral loads. *Computers and Geotechnics.* 24, 89-107.

Taiebat, H. A. & Carter, J. P. 2001. A semi-analytical finite element method for three-dimensional consolidation analysis. *Computer and Geotechnics.* **28**, 55-78.

Taiebat, H. A. & Carter. 2004. Effects of torsion on caisson capacity in clay. *Proc. 9th Australia New Zealand Conference on Geomechanics.* 1, 130-136.

Vesic, A. S. 1975. Bearing capacity of shallow foundations, *Foundation Engineering Handbook*, Eds Winterkorn & Fang, Van Nostrand Reinhold, New York, 121-147.

Watson, P. G., Randolph, M. F. & Bransby, M. F. 2000. Combined lateral and vertical loading of caisson foundations. *Offshore Technology Conference*, Houston, OTC 12195.

Zdravkovic, L., Potts, D. M. & Jardine, R. J. 2001. A parametric study of the pullout capacity of bucket foundations in soft clay. *Géotechnique*, **51**, 1, 55-67.

Zienkiewicz, O. C. and Taylor, R. L. 1989. *The Finite Element Method.* 4th Edition, McGraw-Hill, New York.